12

# Study about controlling and optimizing the power quality in case of nonlinear power loads

Panoiu Manuela and Panoiu Caius
*Polytechnical University of Timişoara*
*România*

## 1. Introduction

An electrical arc furnace EAF transforms the electrical power into thermal power by melting in electric arc furnace the raw materials and wastes. During the arc furnace operation, the random property of arc melting process and the control system are the main reasons of the electrical and thermal dynamics. That will cause serious power quality problems to the supply system, (Andrews et al., 1996), (Wu et al., 2002), (Panoiu et al., 2006), (Panoiu et al., 2007 b). Therefore, the installed power reaches up to 1 MW/t. The AC arc furnace has a non-linear current-voltage characteristic. Therefore it acts as a source of disturbance in the network in which it is supplied. It emits both harmonics and interharmonics and generates voltage unbalances, voltage dips and voltage fluctuations.
However, one of the most substantial disadvantages of arc furnace is caused by the reactive power due to the non-linearity of the electric arc. The significant values of the reactive power cause important losses of active power, therefore the efficiency are affected (Panoiu, 2001), (Panoiu & Panoiu 2007), (Panoiu et al., 2007 c) and (Panoiu et al., 2007 d).
In scope of improving the efficiency of the entire installation it is necessary to use a complex installation for reactive power compensation, harmonics currents filter and load balancing. In order to design such complex installation it is necessary to perform a simulation of the electric arc furnace installation. This simulation is based on the electric arc modelling using PSCAD-EMTDC simulation program. The proposed solution is based on some measurements made at a steel factory in Romania, where there is in function a 100 MVA UHP EAF.

## 2. Measurements on 30 kV line voltage supply

The measurements were made at a 3-phase power supply installation of a 3-phase EAF of 100 t, where is not connected reactive power compensation installation, neither the filters for the harmonic currents or the load balancing device. It is been used a computer with a data acquisition board. All measurements were made on low and medium line voltage supply. In scope of determining the voltages and currents form variations and spectral characteristics of them and also the form variations of quality energy indicators, the measurements were made during the whole duration of process.

The waveforms of the currents and voltages on the low line voltage supply are detailed presented in (Panoiu, 2001) and (Panoiu et al., 2006).
Because our interest is referring to 30 kV line voltage supply, in this chapter are presented the measurements results on this line.
In figure 1 is presented the waveform of the voltage and current in melting phase and in figure 2 the waveform in the phase of stable burning of the electric arc.

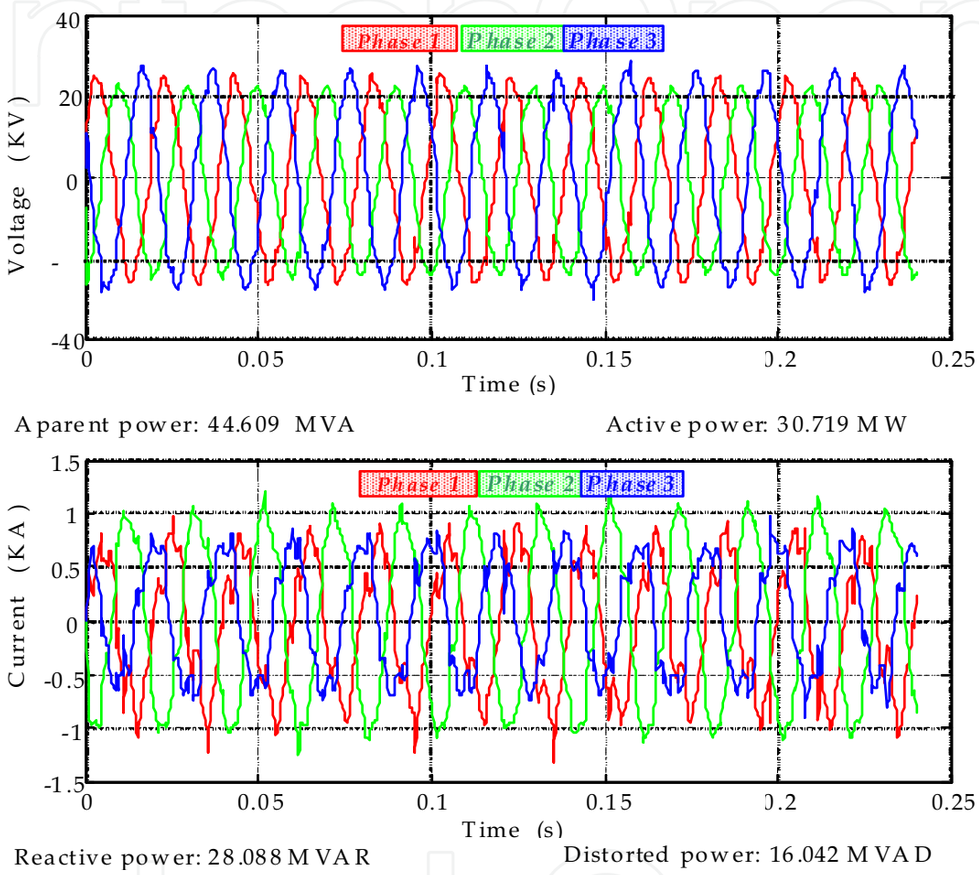


Fig. 1. The voltages and currents time variation on 30 kV line voltage supply in melting phase after 12 minutes from the start of charges.

It can be observed that in the melting phase the voltages and currents are strong distorted. Also, it can be noticed that because the amplitudes of the currents and voltages on the 3 phases are unequal, the load is strongly unbalanced. In the phase of the electric arc stable burning, that appears towards the final of the heat making, especially during the stable burning and reduction (deoxidation) processes, is found that the distortions that appear in the currents and voltages wave forms are more reduced.
The spectral characteristics of the current and voltage, presented in figures 3 and 4, were obtained by using a Matlab program to process the data acquired and using the Fast Fourier Transform. The graphical representations are made from 0 Hz to 1000 Hz, which correspond to a 20$^{th}$ maximum harmonic order.

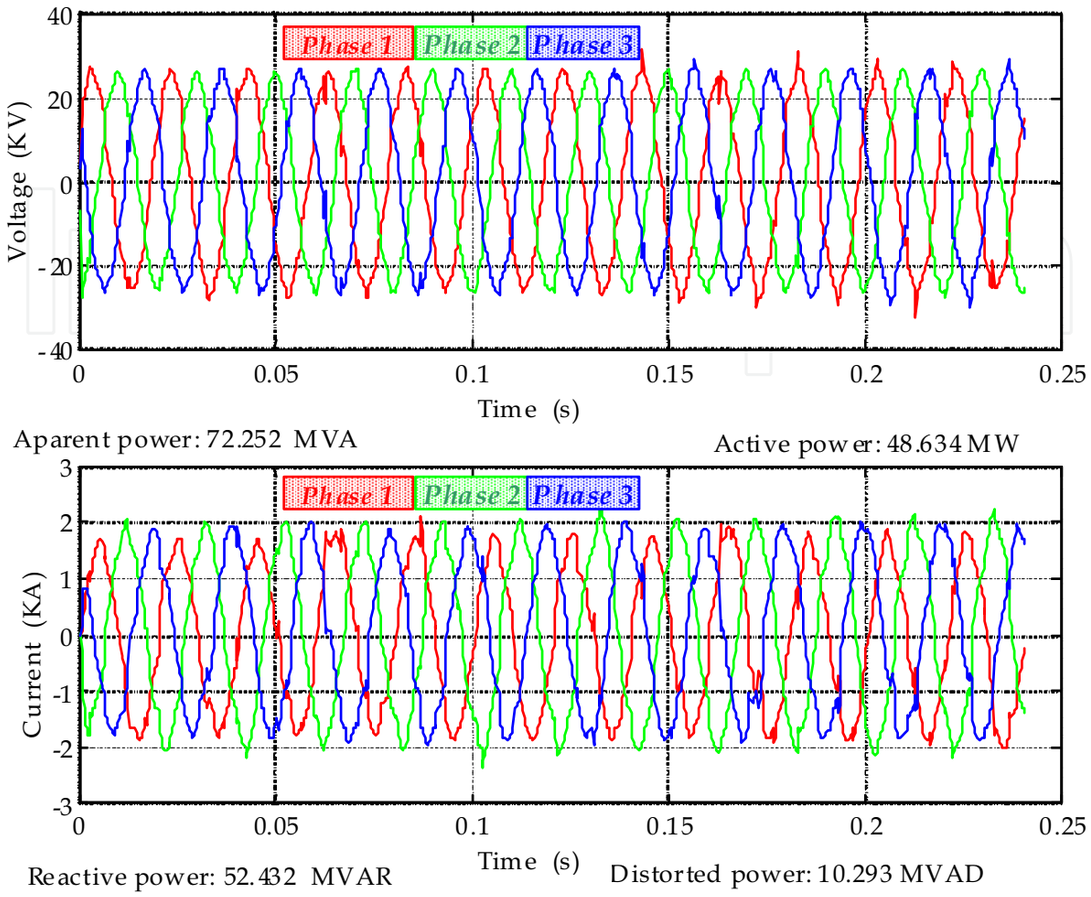


Fig. 2. The voltages and currents time variation on 30 kV line voltage supply in melting phase after 2 hours and 13 minutes from the start of charges.

As regards the voltage on the low voltage line, in the melting phase one can notice the presence of harmonics of 5th, 7th, 11th and 13th order, but also the components of other frequencies than the harmonics (inter-harmonics), while in the oxidation phase is found practically only the presence of the fundamental. This proves that in the melting phase the voltage waveform are much more distorted that in the stable burning phase. In the currents case, is found that in the melting phase is predominant the fundamental frequency component, the other harmonics and inter-harmonics having amplitudes roughly equal, which demonstrates that, in this phase, the current wave is strongly distorted.
In figure 5 is presented the variation of the active and reactive powers on the entire melting process duration. It can be observed that the maximum value is approximately 55 – 60 MW for active power and 50 MVAR for reactive power. These values are used in designing of the reactive power compensation installation and currents harmonic filters.
From the presented above, resulted that, regardless the technological phase, the currents and voltages from the low voltage line are distorted on the entire heat-making duration. Also the unbalanced character of the load it is significant.

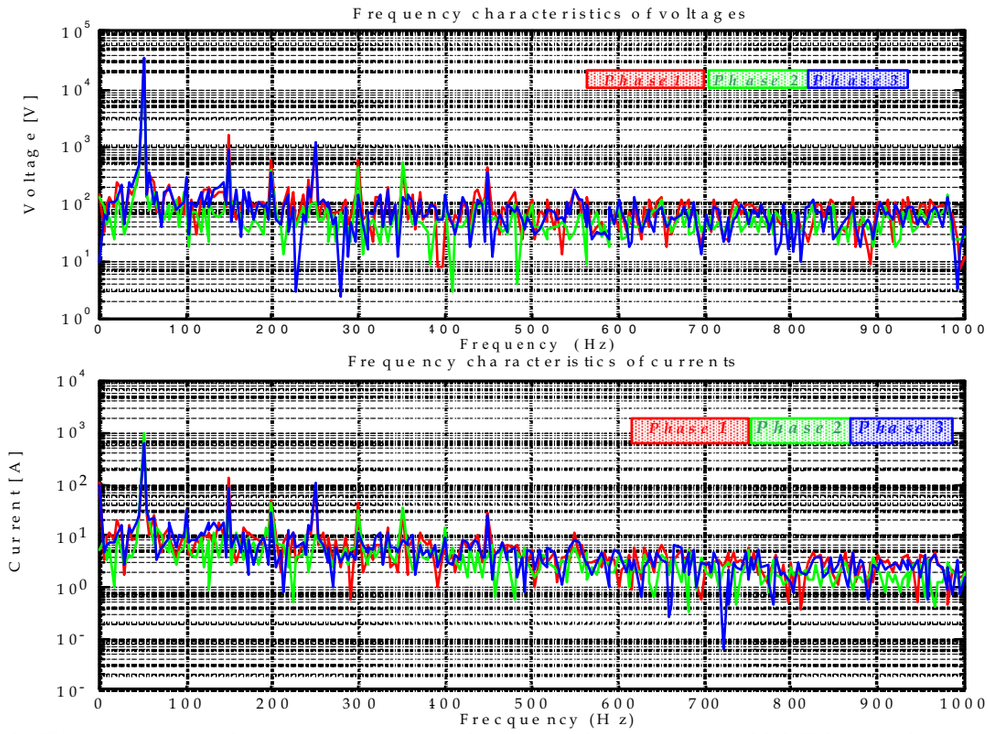


Fig. 3. The frequency characteristics for voltages and currents on 30 kV line voltage supply in melting phase after 12 minutes from the start of melting.

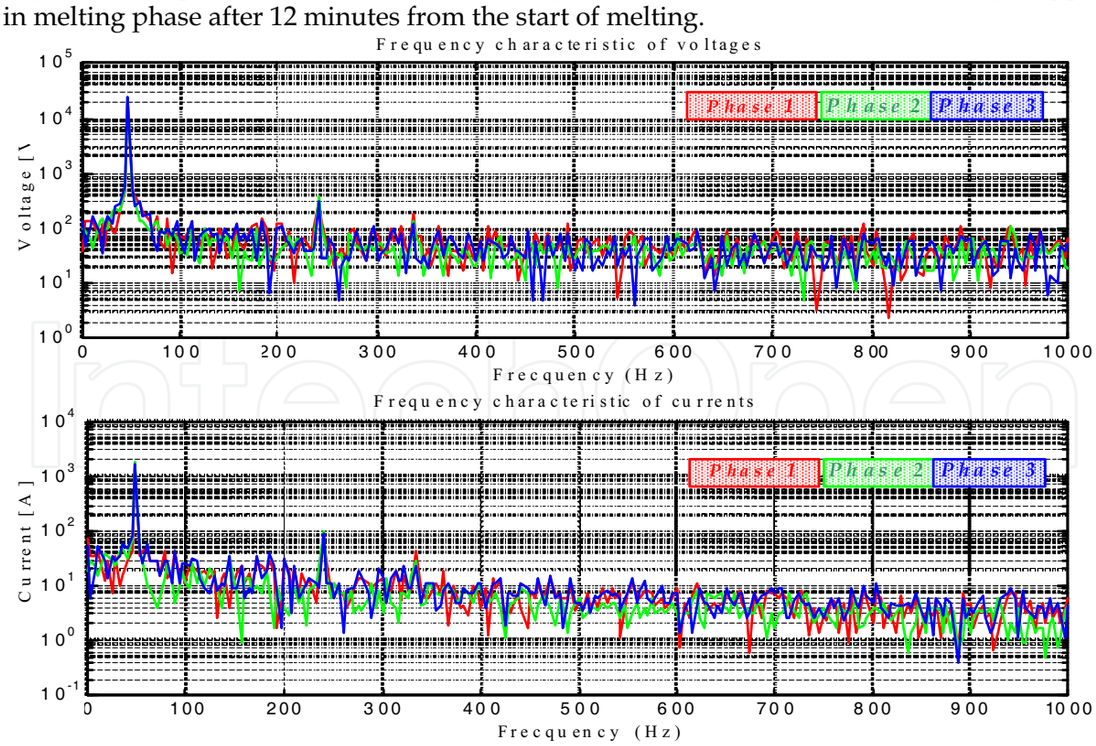


Fig. 4. The frequency characteristics of voltages and currents on 30 kV line voltage supply in melting phase after 2 hours and 13 minutes from the start of melting.

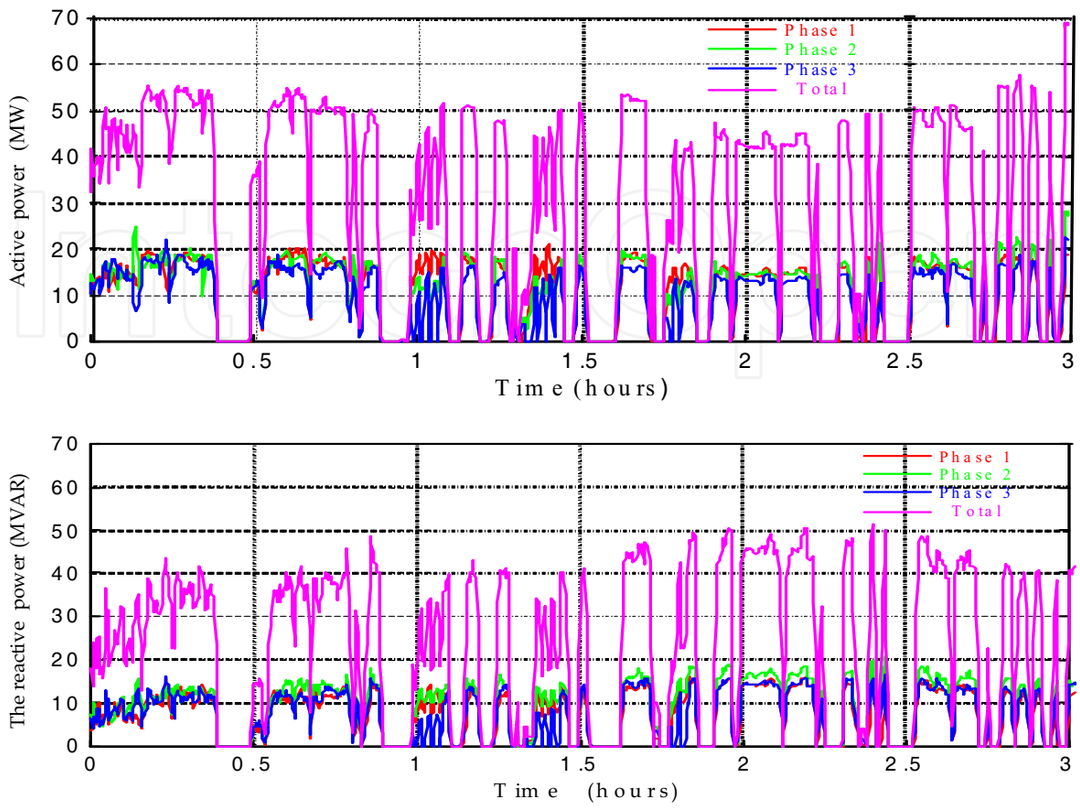


Fig. 5. The variation of the active and reactive powers on the entire melting charge duration.

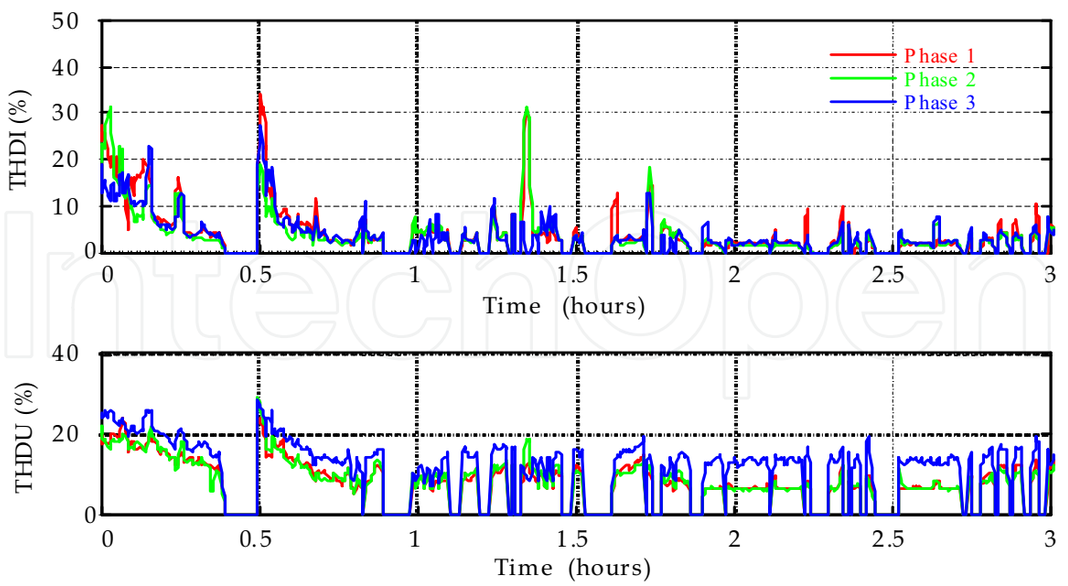


Fig. 6. The variation of the total harmonic distortion of the current and voltage on the entire melting charge duration

In figure 6 is presented the variation form of the total harmonic distortion for the current and voltage waveforms.
There were obtained values between 5 - 25% for total harmonic distortion voltage, respectively 5 - 35%, higher in the melting phase, for the total harmonic distortion current. Comparing these values with the international standards where the value of the permitted total harmonic distortion on the low voltage line is 8% results that these exceed the international standards.

## 3. Simulation of the electrical installation functioning of the electric arc furnace

### 3.1. Models of the electric arc

In (Montanari et al., 1994), (Tang et al., 1997), (Panoiu, 2001), (Boulet et al., 2003), (Cano & Tacca, 2005), (Panoiu & Panoiu, 2006) and (Panoiu & Panoiu, 2007) were presented some models for the electric arc. Studying these models, in this chapter was chosen the model based on the empirical relation between the arc current, arc voltage and arc length. This model, given in (Montanari et al., 1994), (Tang et al., 1997), (Panoiu & Panoiu, 2006) and (Panoiu & Panoiu, 2007), considers the characteristic current-voltage described by relation

$$U_A = U_{th} + \frac{C}{D + I_A} \tag{1}$$

In this relation $U_A$ and $I_A$ are the arc voltage and arc current, and Ud are the threshold voltage. The C and D constants determine the difference between the current increasing part and current decreasing part of the current–voltage characteristic ($C_a$, $D_a$ irrespective $C_b$, $D_b$). The typical values are: $U_d$ = 200 V, $C_a$ = 190000 W, $C_b$ = 39000 W, $D_a$ = $D_b$ = 5000 A (Montanari et al., 1994) and (Tang et al., 1997). Because the real values of the model parameters depend on the voltage arc variations, the dynamic arc voltage–current characteristic must be an arc length function, given by relation (2) in which $U_{A0}$ represent the value of the arc voltage for a reference arc length $l_0$ and k is the ratio between the threshold voltage value for arc length l, $U_{th}(l)$ and the threshold voltage value for arc length $l_0$, $U_{th}(l_0)$.

$$U_A = k \cdot U_{A0}(I_A) \tag{2}$$

The dynamic model for electric arc presumes that the relation between the threshold voltage value and the arc length can be expressed by:

$$U_{th} = A + Bl \tag{3}$$

In (3) A is a constant equal with the sum of cathode and anodic threshold voltages ($A \cong 40V$) and B represent the threshold voltage on the unit length, having usual values of 10 V/cm. The dependency of k by the electric arc length is given by:

$$k(l) = \frac{A + B \cdot l}{A + B \cdot l_0} \tag{4}$$

The PSCAD-EMTDC electrical scheme of the EAF is presented in figure 7.

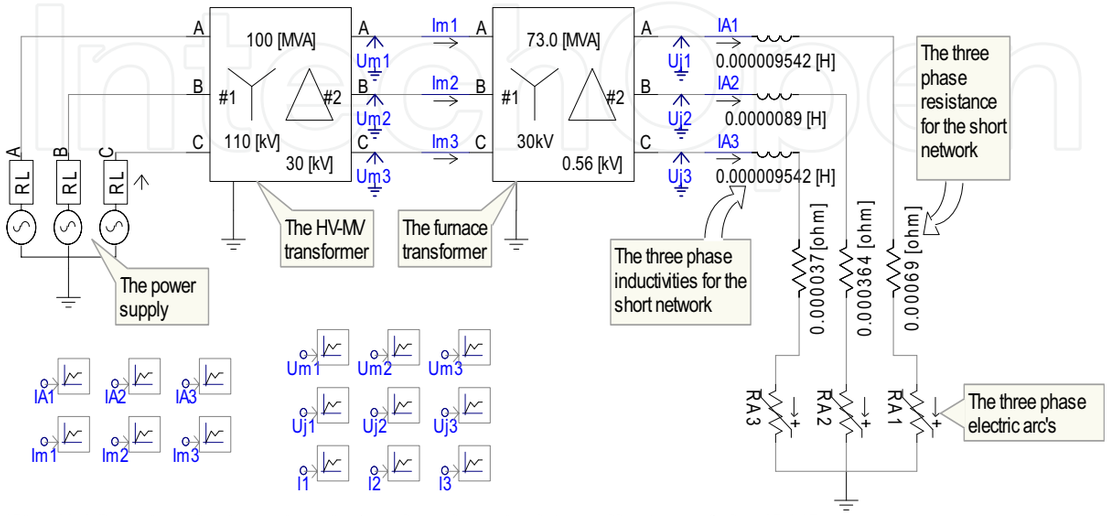


Fig. 7. The simulation circuit for the electrical installation of the EAF.

The parameters of the electrical installation of the EAF were measured on the actual installation at a steel factory. The relation (5) and (6) present the values of the short network parameters. The resistances on each phase are:

$$\begin{aligned} R_{r1} &= 0.6908\,\text{m}\Omega, \\ R_{r2} &= 0.3640\,\text{m}\Omega, \\ R_{r3} &= 0.0372\,\text{m}\Omega, \end{aligned} \tag{5}$$

The total inductivities on each phase are:

$$\begin{aligned} L_{r1} &= L_{r3} = 9.5422\,\mu\text{H} \\ L_{r2} &= 8.9416\,\mu\text{H} \end{aligned} \tag{6}$$

Because the impedances of medium voltage supplying line are small compared with the ones from the low voltage line, these were included in the EAF transformer parameters. The values of the main parameters of the EAF transformer are 73 MVA, 30KV/0,6KV, $\Delta$/Y connections.

### 3.2. The reactive power compensation, harmonics filters and load balancing installation design

To determine the values of the elements of the harmonic filters and reactive power compensation installation it was used the measurement results performed on the installation of the 100 tones electric arc furnace, presented in figure 5.

Starting from these results and taking into consideration the desired power factor of $\cos\Phi = 0.95$, the total reactive power which must be compensated is given by relation (7).

$$Q_{total} = 84.2 \text{ MVAR} \tag{7}$$

The total reactive power which must be compensated is composed by two parts. The first part is the fixed reactive power which is chosen taking into consideration the figure 5 and it is given by relation (8).

$$Q_{const} = 25.8 \text{ MVAR} \tag{8}$$

The fixed reactive power is composed by the reactive power which is obtained on fundamental frequency due to harmonic filters and a reactive power due to the fixed battery. Taking into account the measurements on the 30 kV supplying line feed, the nominal currents for the filters design are $I_n^5 = 100\text{A}$, $I_n^7 = 50\text{A}$, $I_n^{11} = 25\text{A}$ and $I_n^{13} = 25\text{A}$. These values have been determined from measured data using FFT (Fast Fourier Transform). To determine the values of the filters capacitors it is necessary to know the values of the $k^{th}$ order harmonics currents, because, following the standards, a capacitor with a certain nominal voltage $U_{n50}$, corresponding to the fundamental with the frequency of 50 Hz and a certain nominal current $I_{n50}$ can function in a long time distorted regime characterized by $U_{ef} = 1.1 \cdot U_{n50}$ and $I_{ef} = 1.3 \cdot I_{n50}$, which mean a overloading by 43%. For this reason it is important to determine the nominal value for the *k* – harmonic. The harmonic filters were designed using these values and were obtained the component values from figure 8. The reactive power from harmonic filters is given by relation (9) and the reactive power from fixed battery is given from relation (10).

$$Q_F = Q_F^5 + Q_F^7 + Q_F^{11} + Q_F^{13} = 12.53 \text{ MVAR} \tag{9}$$

$$Q_{fixed\ battery} = 13.27 \text{ MVAR} \tag{10}$$

In conclusion the constant reactive pover is composed from four parts due to the harmonic filters and one part due to the fixed battery, as in relation (11).

$$\begin{aligned} Q_F^5 &= 6.785 \text{ MVAR}, \\ Q_F^7 &= 2.494 \text{ MVAR}, \\ Q_F^{11} &= 1.628 \text{ MVAR}, \\ Q_F^{13} &= 1.624 \text{ MVAR}, \\ Q_{fixed\ battery} &= 13.27 \text{ MVAR}. \end{aligned} \tag{11}$$

Knowing the maximum value of the reactive power during the whole charge and the reactive power of the harmonic filters, it can be determined the variable reactive power needed to be compensated. From the condition that the voltage variation to be less then 0.4% result that the number of steps of the fixed reactive power compensation installation is 14. From the value of the variable reactive power, relation (12), result the value of a step reactive power from relation (13).

$$Q_{var} = 58.4 \text{ MVAR} \tag{12}$$

$$\Delta Q_{step} = 4.17 \text{ MVAR} \tag{13}$$

In figure 9 is presented the PSCAD-EMTDC simulation scheme for the electrical installation of the EAF with all improvement power quality installations.

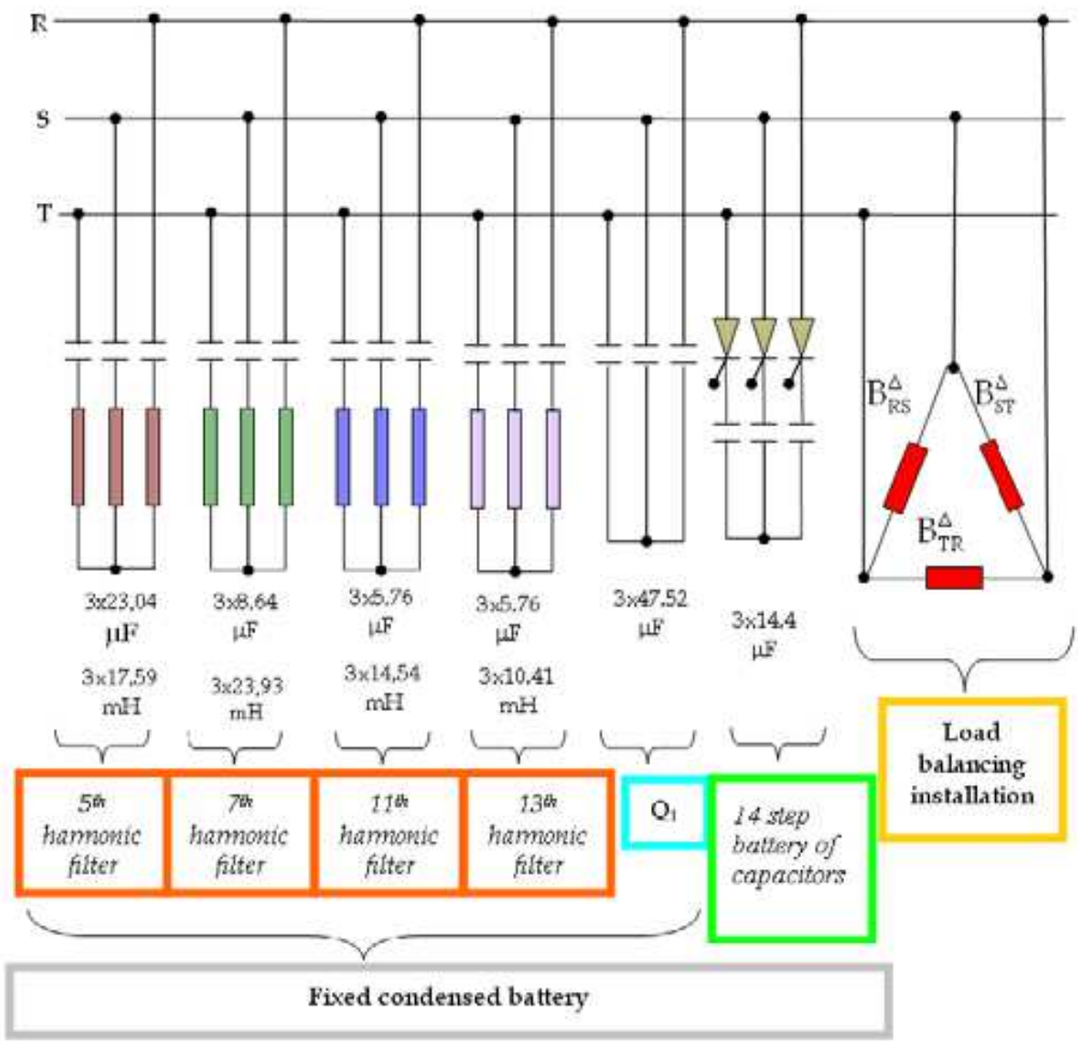


Fig. 8. The scheme of reactive power compensation, harmonics filters and load balancing installation.

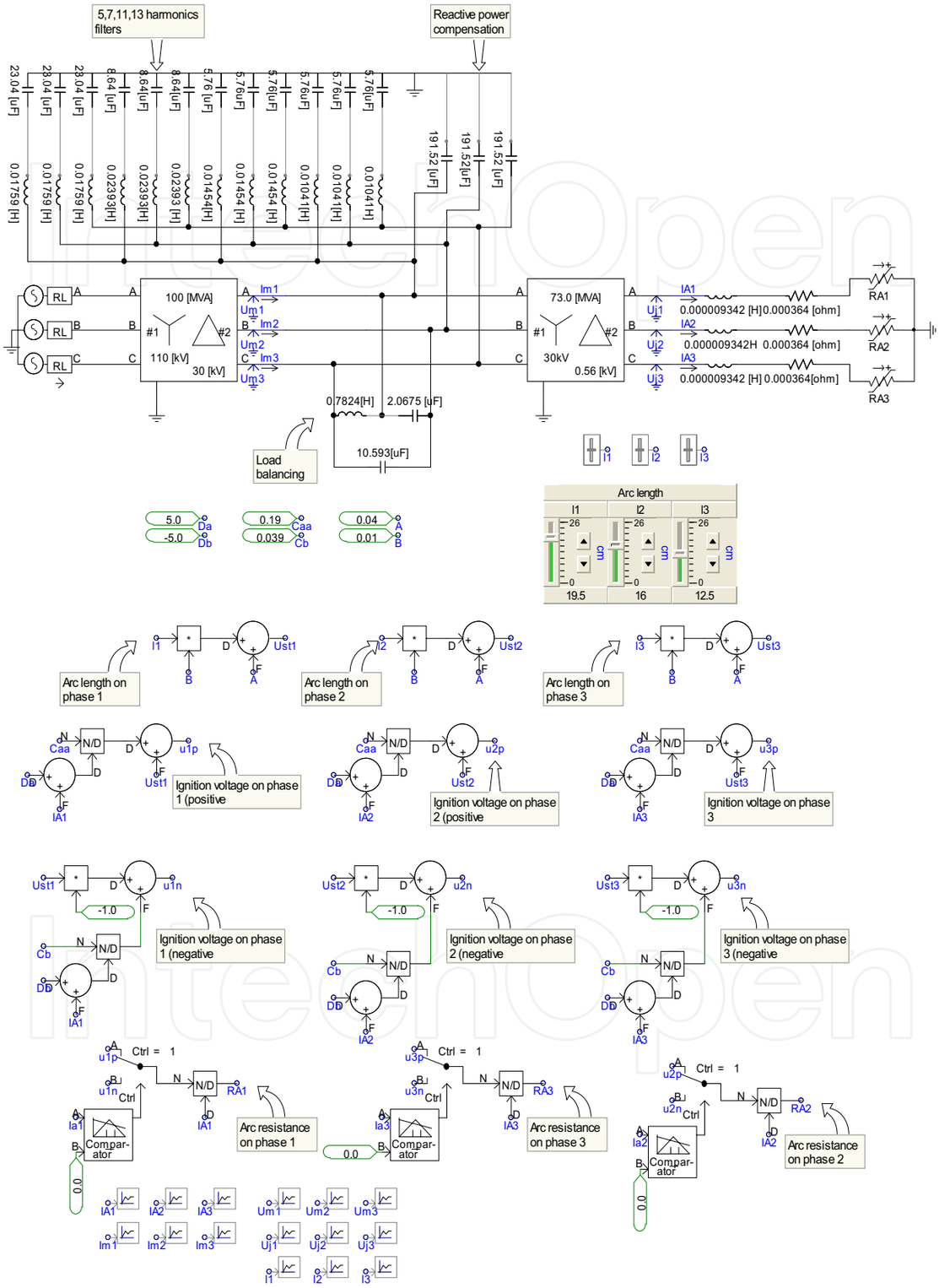


Fig. 9. The PSCAD-EMTDC simulation scheme for the electrical installation of the EAF.

## 4. Simulation results for the UHP EAF

For simulation it was use an electric arc model which is detailed presented in (Panoiu & Panoiu 2007), (Panoiu et al., 2007 a) and (Panoiu et al., 2007 d). In order to obtain conclusions about the effects of reactive power compensation, current harmonics filters and load balancing, simulations were made in five different cases, presented in the next sections.

### 4.1. Simulation results without improving the functioning regime

Because the EAF power supply is made through a 3-phase network with 3 conductors, the homopolar currents that appear have small values, thus they can be neglected. In these conditions, the expression for power factor is given by relation (14) (Buta et al., 1996), (Ionescu & Pop, 1998) and (Buta & Pană, 2000):

$$k_p = \frac{\cos\phi_1^+}{\sqrt{1+k_{ni1}^2\cdot\left(1+\sum_{k=2}^{\infty}\left(\gamma_{I_k}^-\right)^2\right)+\sum_{k=2}^{\infty}\left(\gamma_{I_k}^+\right)^2}} \tag{14}$$

From the analysis of the expression for power factor it found that this emphasizes both the non-symmetric regime, by the asymmetry coefficient $k_{ni1}$, and the non-sinusoidal one, by the level of the harmonic currents of direct and reverse sequence for the harmonics of rank higher than one, $\gamma_{Ik}^-$ and $\gamma_{Ik}^+$ .

As regards the effect of the three elements, meaning the circulation of the reactive power on the fundamental, the unbalance of the currents, respectively their non-sinusoidal upon the loss increasing in the network, this one is different. If it is considered the loss reduction by applying of the three optimization actions as being

$$\frac{\Delta P}{\Delta P_{min}} = \frac{1+k_{ni1}^2\cdot\left(1+\sum_{k=2}^{\infty}\left(\gamma_{I_k}^-\right)^2\right)+\sum_{k=2}^{\infty}\left(\gamma_{I_k}^+\right)^2}{\cos^2\phi_1^+}, \tag{15}$$

it can be established the sensitivity of the loss reduction by each of the reminded actions, calculating the partial derivatives. Thus can be calculated:

- the sensitivity of the loss reduction with load balancing on the fundamental,

$$\frac{\partial\left(\Delta P/\Delta P_{min}\right)}{\partial k_{ni1}} = 2\cdot k_{ni1}\cdot\frac{1+\sum_{k=2}^{\infty}\left(\gamma_{I_k}^-\right)^2}{\cos^2\phi_1^+} \tag{16}$$

- the sensitivity reffering to harmonics atenuation

$$\frac{\partial\left(\Delta P/\Delta P_{min}\right)}{\partial\gamma_{Ik}^-} = \frac{2\cdot k_{ni1}^2\cdot\gamma_{Ik}^-}{\cos^2\phi_1^+} \tag{17}$$

respectively

$$\frac{\partial\left(\Delta P / \Delta P_{min}\right)}{\partial \gamma_{Ik}^{+}} = \frac{2 \cdot \gamma_{Ik}^{+}}{\cos^2 \phi_1^{+}} \tag{18}$$

- the sensitivity against the improvement of the power factor on fundamental:

$$\frac{\partial\left(\Delta P / \Delta P_{min}\right)}{\partial \cos \phi_1^{+}} = -\frac{2}{\cos^3 \phi_1^{+}}\left[1 + k_{ni1}^2 \cdot \left(1 + \sum_{k=2}^{\infty}\left(\gamma_{I_k}^{-}\right)^2\right) + \sum_{k=2}^{\infty}\left(\gamma_{I_k}^{+}\right)^2\right] \tag{19}$$

Studying the usual values of the quantity that are part of the relations (16) - (19), it results that the optimization actions efficiency in power loss reductions is given, in the importance order, by the reactive power compensation for improving the power factor, reducing the harmonics currents and load balancing. In table 1 are presented the results obtained by simulations in conditions where not performed any optimization action.
The presented data were determined by simulation using PSCAD-EMTDC, where the unbalanced regime was obtained for unequal values of the electric arc length (Panoiu et al., 2007 a). The results were obtained based on the data obtained by simulations, using Matlab program.

| | ***The fundamental*** | ***5th harmonic*** | ***7th harmonic*** | ***11th harmonic*** | ***13th harmonic*** |
|---|---|---|---|---|---|
| $\underline{I}_R$ | -458.16-1324.82 j | -18.02+46.25 j | 6.89+26.80 j | -9.58-3.44 j | -8.19+2.20 j |
| $I_R$ | 1401.81 | 49.64 | 27.67 | 10.17 | 8.48 |
| $\underline{I}_S$ | -876.95+1248.53 j | -27.63-16.91 j | 6.80-24.86 j | 0.83-3.00 j | 7.07-1.39 j |
| $I_S$ | 1525.73 | 32.39 | 25.77 | 3.11 | 7.21 |
| $\underline{I}_T$ | 1335.10+76.29 j | 45.65-29.34 j | -13.69-1.94 j | 8.75+6.43 j | 1.11-0.81 j |
| $I_T$ | 1337.28 | 54.27 | 13.82 | 10.86 | 1.38 |
| $\underline{I}^+$ | -567.17-1300.31 j | -12.53+1.93 j | 10.07+19.39 j | -1.99-3.97 j | -3.92+2.85 j |
| $I^+$ | 1418.62 | 12.68 | 21.85 | 4.44 | 4.84 |
| $\underline{I}^-$ | 109.48-23.63 j | -5.54+44.34 j | -3.20+7.59 j | -7.55+0.58 j | -4.32-0.59 j |
| $I^-$ | 112.00 | 44.68 | 8.24 | 7.57 | 4.36 |
| $\underline{I}^0$ | (-1+7 j)4e-013 | (-4.5-5 j)e-013 | (2.5-4 j)e-013 | (-8-1.8 j)e-013 | (-3.5-2 j)e-013 |
| $I^0$ | 7.41e-013 | 6.7328e-013 | 4.58e-013 | 8.11e-013 | 4.07e-013 |
| $k_{ni}$ [%] | 7.90 | 352.32 | 37.70 | 170.58 | 90.11 |
| $k_{nu}$[%] | 0.05 | 368.09 | 37.50 | 191.39 | 85.77 |
| $\gamma_{IkR}$ | 0.98815 | 0.03499 | 0.01950 | 0.00717 | 0.00598 |
| $\gamma_{IkS}$ | 1.07550 | 0.02283 | 0.01817 | 0.00219 | 0.00508 |
| $\gamma_{IkT}$ | 0.94266 | 0.03825 | 0.00974 | 0.00765 | 0.00097 |
| $\gamma_{UkR}$ | 1.00036 | 0.00092 | 0.00062 | 0.00026 | 0.00024 |
| $\gamma_{UkS}$ | 0.99946 | 0.00061 | 0.00056 | 0.00010 | 0.00020 |
| $\gamma_{UkT}$ | 1.00017 | 0.00100 | 0.00031 | 0.00028 | 0.00004 |

Table 1. Simulations results without reactive power compensation, load balancing and harmonics filtering.

Analyzing the presented results is found that:

- the power supply system is unbalanced, fact which results from the values of the asymmetry coefficients of currents and voltages (much higher for harmonics) and due to the high value of the reverse sequence component of the current, both for fundamental, 112 A, and for harmonics. It must be noticed that the 5th harmonic has the effective value of the reverse sequence current of 44.68 A.
- the EAF is an important harmonics generator in the power supply line, which results from the high values of direct sequence currents, respectively reverse sequence of the harmonics of rank 5, 7, 11 and 13. Also is found an important unbalance of the harmonic currents, especially for the 5th harmonic.
- the values of the homopolar currents obtained following simulations are very small, fact which justifies the previously made approximations.

In figure 10 are represented the phasors of currents and voltages, as well as of their components of direct and reverse sequence.

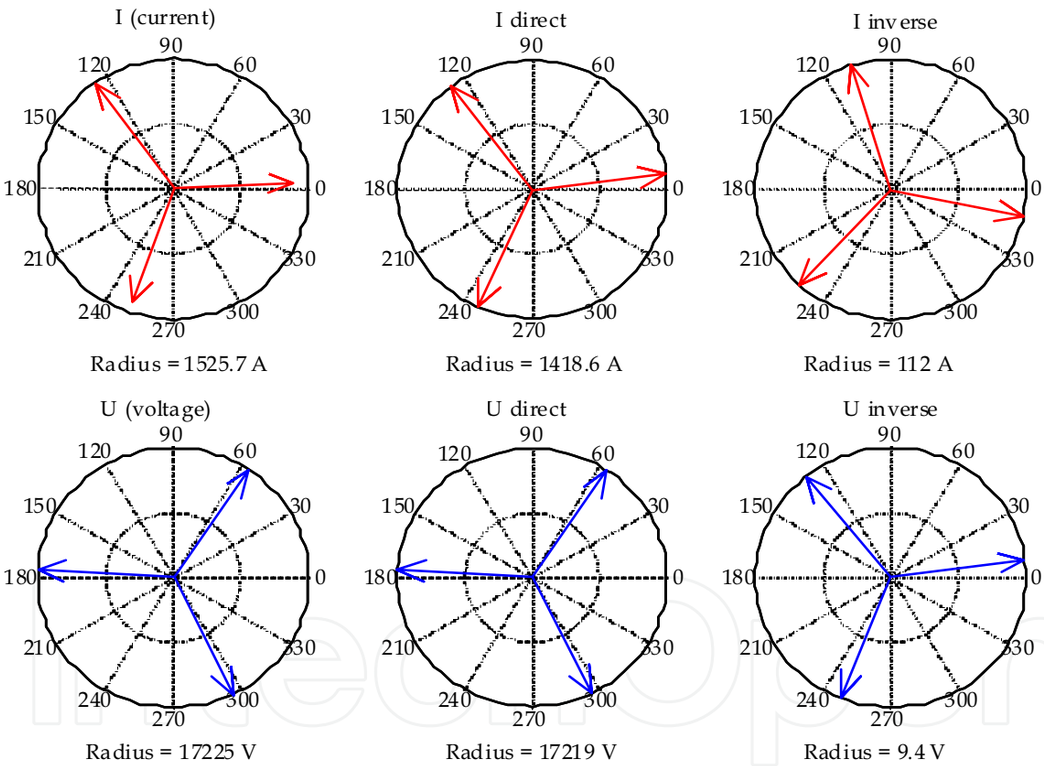


Fig. 10. Current and voltage phasors without any quality energy improvement action

### 4.2. Simulation results with reactive power compensation

In this situation is not taken into account the presence of the unbalanced and non-sinusoidal regime, for the improvement of the power factor being made a symmetrical transversal capacitive compensation. The values of the compensation currents, the same on each phase, are determined from the cancelling condition of the reactive component of the direct sequence current corresponding to the fundamental, which leads to $\cos\phi_1^{+c} = 1$, i.e.

$$I_m\left(\underline{I}_1^{+c}\right)=0 \tag{20}$$

The Y compensator designing is made starting from the currents and voltages values, from table 1, resulted following simulation of electrical installation operation for which was not performed any optimization action. These values are

$$\begin{aligned} \underline{I}_R &= -458.2-1342.8\ \text{j A} & \underline{U}_R &= 7598-15459\ \text{j V}\\ \underline{I}_S &= -876.9+1248.5\ \text{j A} & \underline{U}_S &= -17172+143.5\ \text{j V}\\ \underline{I}_T &= 1335.1+76.3\ \text{j A} & \underline{U}_T &= 9574.1+4315\ \text{j V} \end{aligned} \tag{21}$$

Based on these results the currents and voltages direct sequence components (Buta et al., 1996) and (Buta & Pană, 2000) are given by:

$$\begin{aligned} \underline{I}^{+} &= -567.16-1300.3\ \text{j} = 1418.6\cdot e^{-\text{j}\,113.56^{\circ}}\\ \underline{U}^{+} &= 7601.5-15450.7\ \text{j} = 17219\cdot e^{-\text{j}\,63.80^{\circ}} \end{aligned} \tag{22}$$

The value of the capacity, necessary for compensation, results from the cancelling condition of the reactive component for direct current, is given by relation:

$$C^{Y}=\frac{I^{+}\cdot\sin\left(\underline{I}^{+},\underline{U}^{+}\right)}{\omega U^{+}}=200.18\ \mu\text{F}. \tag{23}$$

The **s**imulations performed on the step most closely to the value given by (23)**,** for the compensation installation previously calculated, $C_1^{Y}=205.92\ \mu\text{F}$, have shown that on this step is not succeeding a total cancelling of the reactive component for direct current, the phase difference being $\Delta\phi_1=-1.4422^{\circ}$.

Making simulations on the previous step, $C_2^{Y}=191.52\ \mu\text{F}$, it was found that the phase difference increased to the value $\Delta\phi_2=3.4229^{\circ}$, with inductive character. Even if further to an iterative process was found that the optimal value for capacity, for which is obtained a null phase difference, is $C_{optim}^{Y}=201.7\ \mu\text{F}$, close to the value given by the relation (23), the results of the compensation action, presented in table 2**,** are the ones obtained at the operation on the optimal step of the compensation installation, where $C_1^{Y}=205.92\ \mu\text{F}$.

In case of reactive power compensation, it should not intervene upon the reverse component of the current on fundamental, but, in return, the direct sequence component is reduced from $I_1^{+}$ to $I_1^{+c}=I_1^{+}\cdot\cos\phi_1^{+}=\text{Re}\left(\underline{I}_1^{+}\right)$, $I_1^{+}$ respectively $\cos\phi_1^{+}$ being the direct current, respectively the power factor on fundamental. In accordance, the asymmetry coefficient on fundamental, after compensation, becomes

$$k_{ni1} = \frac{I_1^-}{I_1^+ \cdot \cos\phi_1^+} \tag{24}$$

It can be observed that the asymmetry coefficient on fundamental is increasing the smaller is the power factor before compensation. In case of reactive power compensation the non-symmetry regime is emphasizing.

| | *The fundamental* | *5th harmonic* | *7th harmonic* | *11th harmonic* | *13th harmonic* |
|---|---|---|---|---|---|
| $\underline{I}_R$ | 537.55-842.88 j | -15.01+51.92 j | 13.06+28.78 j | -12.11-0.02 j | -7.79+7.00 j |
| $I_R$ | 999.70 | 54.04 | 31.61 | 12.11 | 10.47 |
| $\underline{I}_S$ | -955.84+147.55 j | -31.90-15.42 j | 2.71-29.00 j | -0.58-3.79 j | 6.93-5.35 j |
| $I_S$ | 967.16 | 35.43 | 29.13 | 3.83 | 8.76 |
| $\underline{I}_T$ | 418.29+695.33 j | 46.91-36.50 j | -15.77+0.22 j | 12.69+3.81 j | 0.86-1.65 j |
| $I_T$ | 811.45 | 59.44 | 15.77 | 13.25 | 1.86 |
| $\underline{I}^+$ | 427.36-817.82 j | -13.45+3.34 j | 15.04+19.79 j | -3.85-3.80 j | -2.80+5.31 j |
| $I^+$ | 922.75 | 13.86 | 24.86 | 5.41 | 6.00 |
| $\underline{I}^-$ | 109.57-24.91 j | -1.53+48.75 j | -2.01+8.95 j | -8.32+3.84 j | -4.96+1.69 j |
| $I^-$ | 112.37 | 48.78 | 9.17 | 9.16 | 5.24 |
| $\underline{I}^0$ | (2.7-2.4 j)e-013 | (-6.5-5 j)e-013 | (-1-1.5 j)e-013 | (3.7-7 j)e-013 | (7.5-7 j)e-013 |
| $I^0$ | 3.6e-013 | 8.1e-013 | 1.9e-013 | 7.7e-013 | 1.009e-012 |
| $k_{ni}$ [%] | 12.18 | 351.98 | 36.89 | 169.49 | 87.34 |
| $k_{nu}$[%] | 0.05 | 350.09 | 36.97 | 166.46 | 87.96 |
| $\gamma_{IkR}$ | 1.08340 | 0.05857 | 0.03425 | 0.01312 | 0.01135 |
| $\gamma_{IkS}$ | 1.04813 | 0.03839 | 0.03157 | 0.00415 | 0.00949 |
| $\gamma_{IkT}$ | 0.87939 | 0.06441 | 0.01709 | 0.01436 | 0.00202 |
| $\gamma_{UkR}$ | 1.00037 | 0.00100 | 0.00068 | 0.00030 | 0.00027 |
| $\gamma_{UkS}$ | 0.99947 | 0.00065 | 0.00063 | 0.00010 | 0.00023 |
| $\gamma_{UkT}$ | 1.00016 | 0.00109 | 0.00034 | 0.00033 | 0.00004 |

Table 2. Simulations results using only reactive power compensation.

In figure 11 there were represented the phasors of the fundamental currents and voltages, as well as of the direct and reverse sequence components. Is found that, on one side, the current and voltage phasors for the direct sequence are in phase, but also a decreasing of the value of current combined with the increase of the value of voltage.

### 4.3. Simulation results with load balancing

In this situation it does intervene upon the load balancing without aiming the improvement of the power factor or harmonics decrease. Compensation is non-symmetrical and is possible by means of a circuit in Δ connection, which contains only susceptances, connected in parallel with the mains, in the section where the balancing is desired. This method consists in the computing of element for the load balancing installation using the current and voltage values obtained after the best compensation of the reactive power, the balancing installation being in this case a compensator in Δ conection that can compensate totally the reactive power difference.

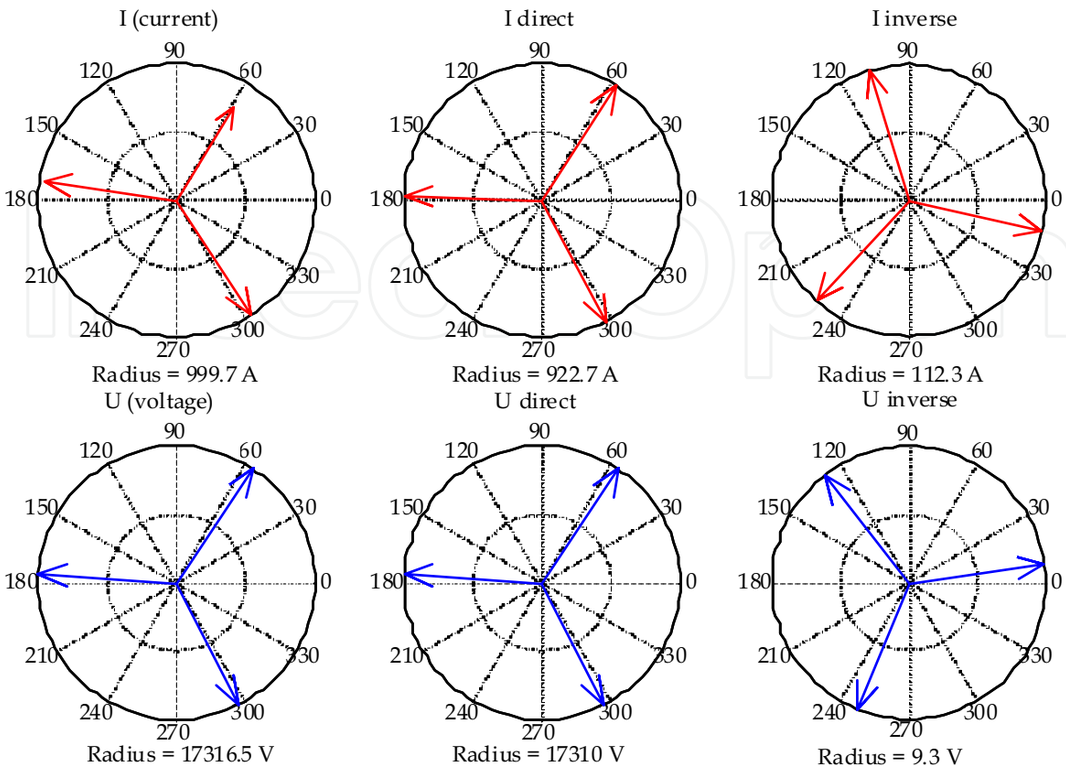


Fig. 11. Current and voltage phasors using only reactive power compensation

The advantages of the proposed method consist in:

- reactive power compensator assembly – balancing installation which has the same performances as a reactive power total compensator together with a balancing installation which does not consume reactive power;
- the load balancing installation, even if it consumes reactive power, has so small values of elements that the thyristors from the structure will not be overloaded. In these conditions it can be achieved also a continuous tunning of the compensators reactive power.

The computing of the balancing installation starts from determination of the currents and voltages values in case of the best reactive power compensation, using the optimal value of the a compensation capacity $C^{Y}_{optim} = 201.7\ \mu F$. These values were obtained based on the data resulted following simulation, being given by the relations

$$\begin{aligned}
\underline{I}^{S}_{R} &= 516.93 - 852.41\ j\ A \\
\underline{I}^{S}_{S} &= 952.32 + 167.66\ jA \\
\underline{I}^{S}_{T} &= 435.39 + 684.74\ j\ A \\
\underline{U}^{S}_{R} &= \quad 7624.4 - 15547\ j\ V \\
\underline{U}^{S}_{S} &= -17260 + 1163.9\ j\ V \\
\underline{U}^{S}_{T} &= \quad 9635.6 + 4381\ j\ V
\end{aligned} \tag{25}$$

Based on (25) it can be computed the load admittances in Y connection

$$\begin{aligned}
\underline{Y}_R^S &= G_R\text{-}jB_R = 0.057343 + 0.005128\,j = 0.057572 \cdot e^{j\,5.1102^\circ} \\
\underline{Y}_S^S &= G_S\text{-}jB_S = 0.055577 - 0.005966\,j = 0.055896 \cdot e^{-j\,6.1270^\circ} \\
\underline{Y}_T^S &= G_T\text{-}jB_T = 0.046861 + 0.001123\,j = 0.046875 \cdot e^{j\,1.3728^\circ}
\end{aligned} \tag{26}$$

It is found the presence of an unbalance regarding the modules of the three admittances, while their phases are very small, fact which shows that it was achieved a correct compensation. Based on the load admittances values in Y connection, it can be determined the load admittances values in $\Delta$ connection according to the relations provided in (Buta & Pană, 2000).

$$\begin{aligned}
G_{RS}^S &= \frac{1}{6}\left[\left(G_R + G_S\right) + \frac{1}{\sqrt{3}}\left(B_S - B_R\right)\right] = 0.01988773 \\
B_{RS}^S &= \frac{1}{6}\left[\left(B_R + B_S\right) + \frac{1}{\sqrt{3}}\left(G_R - G_S\right)\right] = 0.00030963 \\
G_{TR}^S &= \frac{1}{3}\left[G_R + \frac{1}{\sqrt{3}}\left(B_R - B_S\right)\right] = 0.01697944 \\
B_{TR}^S &= \frac{1}{3}\left[B_R + \frac{1}{\sqrt{3}}\left(G_S - G_R\right)\right] = -0.00204928 \\
G_{ST}^S &= \frac{1}{3}\left[G_S + \frac{1}{\sqrt{3}}\left(B_R - B_S\right)\right] = 0.01639071 \\
B_{ST}^S &= \frac{1}{3}\left[B_S + \frac{1}{\sqrt{3}}\left(G_S - G_R\right)\right] = 0.00164883
\end{aligned} \tag{27}$$

Designing of the compensator in $\Delta$ connection is made based on the cancelling conditions of the reverse sequence current, according to the relation (24) and also cancelling the reactive power absorbed from the mains. This leads to the equations system

$$\begin{aligned}
&-G_{RS} + 2G_{ST} - G_{TR} + \sqrt{3}\left(B_{TR} - B_{RS}\right) = 0 \\
&\sqrt{3}\left(G_{TR} - G_{RS}\right) + B_{RS} - 2B_{ST} + B_{TR} = 0 \\
&G_{RS} - G_{TR} - \sqrt{3}\left(B_{RS} + B_{TR}\right) = 0
\end{aligned} \tag{28}$$

In (28) was used the notations from (29), where the exponent $^S$ define the load elements and the exponent $^\Delta$ defines the compensator elements. Solving the equations system (28) and considering as unknown the compensator susceptances there were obtained the values from (30).

$$\begin{aligned}
G_{RS} &= G_{RS}^S & G_{ST} &= G_{ST}^S & G_{TR} &= G_{TR}^S \\
B_{RS} &= B_{RS}^S + B_{RS}^\Delta\,, & B_{ST} &= B_{ST}^S + B_{ST}^\Delta\,, & B_{TR} &= B_{TR}^S + B_{TR}^\Delta\,,
\end{aligned} \tag{29}$$

$$B_{RS}^{\Delta} = -B_{RS}^{S} + \frac{1}{\sqrt{3}}\left(G_{ST}^{S} - G_{TR}^{S}\right) = -0.00064953$$
$$B_{ST}^{\Delta} = -B_{ST}^{S} + \frac{1}{\sqrt{3}}\left(G_{TR}^{S} - G_{SR}^{S}\right) = -0.00332793 \quad (30)$$
$$B_{TR}^{\Delta} = -B_{TR}^{S} + \frac{1}{\sqrt{3}}\left(G_{RS}^{S} - G_{ST}^{S}\right) = 0.00406828$$

In this case the compensator in $\Delta$ connection has the elements

$$C_{RS} = 2.0675 \ \mu F$$
$$C_{ST} = 10.5931 \ \mu F \quad (31)$$
$$L_{TR} = 0.7824 \ H$$

With these values, following the performed simulations, it was obtained the results presented in table 3.

| | *The fundamental* | *5th harmonic* | *7th harmonic* | *11th harmonic* | *13th harmonic* |
|---|---|---|---|---|---|
| $\underline{I}_R$ | -567.81-1300.14 j | -17.94+46.50 j | 6.93+26.98 j | -9.60-3.30 j | -8.21+2.37 j |
| $I_R$ | 1418.72 | 49.84 | 27.86 | 10.15 | 8.55 |
| $\underline{I}_S$ | -844.92+1143.65 j | -27.99-16.50 j | 6.61-25.54 j | 0.37-2.89 j | 7.21-1.92 j |
| $I_S$ | 1421.91 | 32.49 | 26.38 | 2.92 | 7.46 |
| $\underline{I}_T$ | 1412.73+156.49 j | 45.93-30.01 j | -13.54-1.44 j | 9.23+6.19 j | 1.00-0.45 j |
| $I_T$ | 1421.37 | 54.86 | 13.62 | 11.11 | 1.10 |
| $\underline{I}^+$ | -568.51-1301.39 j | -12.81+1.80 j | 10.41+19.33 j | -2.11-4.22 j | -3.68+2.95 j |
| $I^+$ | 1420.15 | 12.93 | 21.95 | 4.72 | 4.71 |
| $\underline{I}^-$ | 1.15+1.43 j | -5.22+44.54 j | -3.53+7.67 j | -7.44+0.85 j | -4.56-0.65 j |
| $I^-$ | 1.83 | 44.85 | 8.44 | 7.49 | 4.60 |
| $\underline{I}^0$ | (2.2-1.2 j)e-013 | (-4.7-6 j)e-013 | (9+9.1 j)e-013 | (7.3+3 j)e-013 | (6.4+4.4 j)e-014 |
| $I^0$ | 2.5e-013 | 7.6e-013 | 1.3e-012 | 7.9e-013 | 6.4e-013 |
| $k_{ni}$ [%] | 0.13 | 346.75 | 38.45 | 158.66 | 97.65 |
| $k_{nu}$[%] | 0.00 | 371.23 | 39.34 | 193.33 | 96.09 |
| $\gamma_{IkR}$ | 0.99900 | 0.03510 | 0.01962 | 0.00715 | 0.00602 |
| $\gamma_{IkS}$ | 1.00124 | 0.02288 | 0.01858 | 0.00205 | 0.00525 |
| $\gamma_{IkT}$ | 1.00086 | 0.03863 | 0.00959 | 0.00782 | 0.00077 |
| $\gamma_{UkR}$ | 1.00001 | 0.00092 | 0.00062 | 0.00026 | 0.00024 |
| $\gamma_{UkS}$ | 0.99998 | 0.00062 | 0.00057 | 0.00010 | 0.00020 |
| $\gamma_{UkT}$ | 1.00000 | 0.00101 | 0.00029 | 0.00028 | 0.00003 |

Table 3. Simulation results using only load balancing.

Analyzing the obtained results it can conclude the following:

- the reverse sequence currents value is very small, fact which demonstrates that it was achieved a good load balancing;
- as regards the currents on the three phases, is found a very good symmetry on the fundamental of the currents of the three phases;

- the asymmetry factor is much reduced compared with the version where there was not action for power quality improvement, presented in table 1;

In figure 12 are represented the currents and voltages phasors as well as of direct and reverse sequence components.

As in case of reactive power compensation, it was a matter of finding some values of the load balancing installation for which should be obtained a value as smaller of the current's reverse sequence component. Following an iterative process, it was found that the optimal values of the balancing installation are given from relation (32), for which was obtained an effective value of the reverse sequence current of $I^{-} = 0.8752A$, smaller than the one presented in table 3.

$$\begin{aligned} C_{RS,optim} &= 2.10 \ \mu F \\ C_{ST,optim} &= 10.60 \ \mu F \\ L_{TR,optim} &= 0.79 \ H \end{aligned} \tag{32}$$

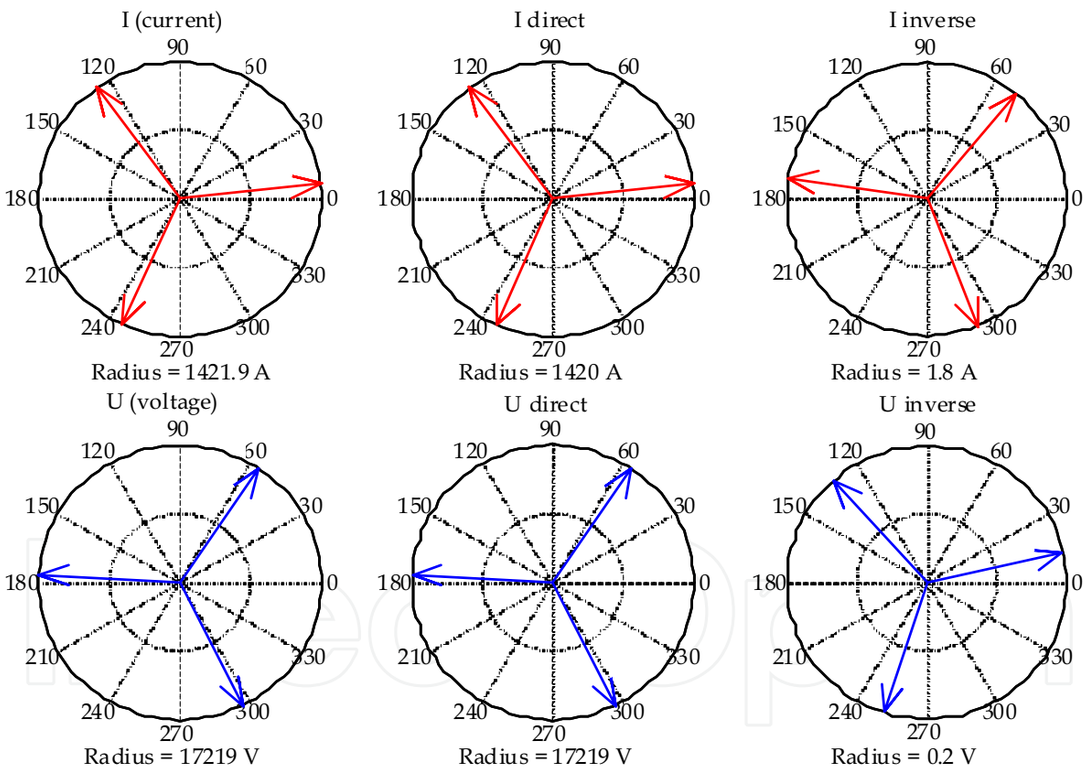


Fig. 12. Current and voltage phasors using only load balancing

### 4.4. Simulation results with currents harmonics filtering

The filtration of current harmonics is achieved using filters of pass-band type of rank I (Chiuță & Conecini, 1989). Taking into account that normally the main harmonics of the current and voltage are the ones of rank 5, 7, 11 and 13, the analysis of the filters influence was made using the values determined for these filters.

It is known that the dimensioning of resonant circuits can be made based on two criteria, (Chiuță & Conecini, 1989), (Buta & Pană, 2000):

- for circuits in with filtration has the main role;
- for double scope circuits, compensation – filtration.

In case of the filters designed resulted that the calculated filters delivers reactive power on fundamental, see relation (11), in such way that in case of a consumer with inductive character is expected to contribute also to the improvement of the power factor of the consumer-filter unit.

Following the performed simulations using simultaneously the 4 harmonic filters, there were obtained the results presented in table 4, based on which is found as follows:

- the harmonic currents values are strongly diminished, both for the direct sequence component and also for the inverse sequence one;
- because the capacitors disposal on the three phases are identical, it results a compensation of the direct sequence component of the load current.

From this reason results a decrease of their effective values and an emphasizing of the non-symmetry of currents, fact which results also from the values of the non-symmetry coefficients on fundamental.

| | ***The fundamental*** | ***5th harmonic*** | ***7th harmonic*** | ***11th harmonic*** | ***13th harmonic*** |
|---|---|---|---|---|---|
| $\underline{I}_R$ | -167.25-1225.60 j | 3.29+6.77 j | 5.99+5.25 j | -3.09+0.09 j | -1.93+1.11 j |
| $I_R$ | 1236.96 | 7.53 | 7.96 | 3.09 | 2.22 |
| $\underline{I}_S$ | -947.08+947.05 j | -3.57+1.40 j | -2.35-7.21 j | -0.12-1.05 j | 1.84-0.94 j |
| $I_S$ | 1339.35 | 3.84 | 7.59 | 1.05 | 2.07 |
| $\underline{I}_T$ | 1114.33+278.56 j | 0.28-8.17 j | -3.64+1.97 j | 3.21+0.96 j | 0.09-0.16 j |
| $I_T$ | 1148.62 | 8.18 | 4.14 | 3.35 | 0.18 |
| $\underline{I}^+$ | -276.93-1207.51 j | -1.84+1.05 j | 5.57+2.90 j | -1.06-0.95 j | -0.82+1.01 j |
| $I^+$ | 1238.86 | 2.11 | 6.28 | 1.43 | 1.30 |
| $\underline{I}^-$ | 109.48-17.23 j | 5.14+4.65 j | 0.45+2.32 j | -2.09+0.96 j | -1.11+0.07 j |
| $I^-$ | 110.83 | 6.93 | 2.36 | 2.30 | 1.11 |
| $\underline{I}^0$ | (-6-1.7 j)e-013 | (-5.4-1.2 j)e-013 | (1-3.3 j)e-013 | (-7.3-1.2 j)e-013 | (3-4.2 j)e-013 |
| $I^0$ | 6.2e-013 | 5.6e-013 | 3.5e-013 | 7.4e-013 | 5.2e-013 |
| $k_{ni}$ [%] | 8.95 | 327.85 | 37.67 | 161.36 | 85.80 |
| $k_{nu}$[%] | 0.11 | 1129.99 | 43.48 | 608.33 | 59.92 |
| $\gamma_{IkR}$ | 0.99847 | 0.00608 | 0.00643 | 0.00250 | 0.00179 |
| $\gamma_{IkS}$ | 1.08111 | 0.00310 | 0.00612 | 0.00085 | 0.00167 |
| $\gamma_{IkT}$ | 0.92716 | 0.00660 | 0.00334 | 0.00270 | 0.00015 |
| $\gamma_{UkR}$ | 1.00075 | 0.00034 | 0.00048 | 0.00025 | 0.00026 |
| $\gamma_{UkS}$ | 0.99894 | 0.00021 | 0.00038 | 0.00019 | 0.00020 |
| $\gamma_{UkT}$ | 1.00031 | 0.00026 | 0.00024 | 0.00021 | 0.00010 |

Table 4. Simulation results using only current harmonics filtering.

In figure 13 are presented the phasors of the fundamental frequency currents and voltages, as well as of their direct and inverse sequence components.

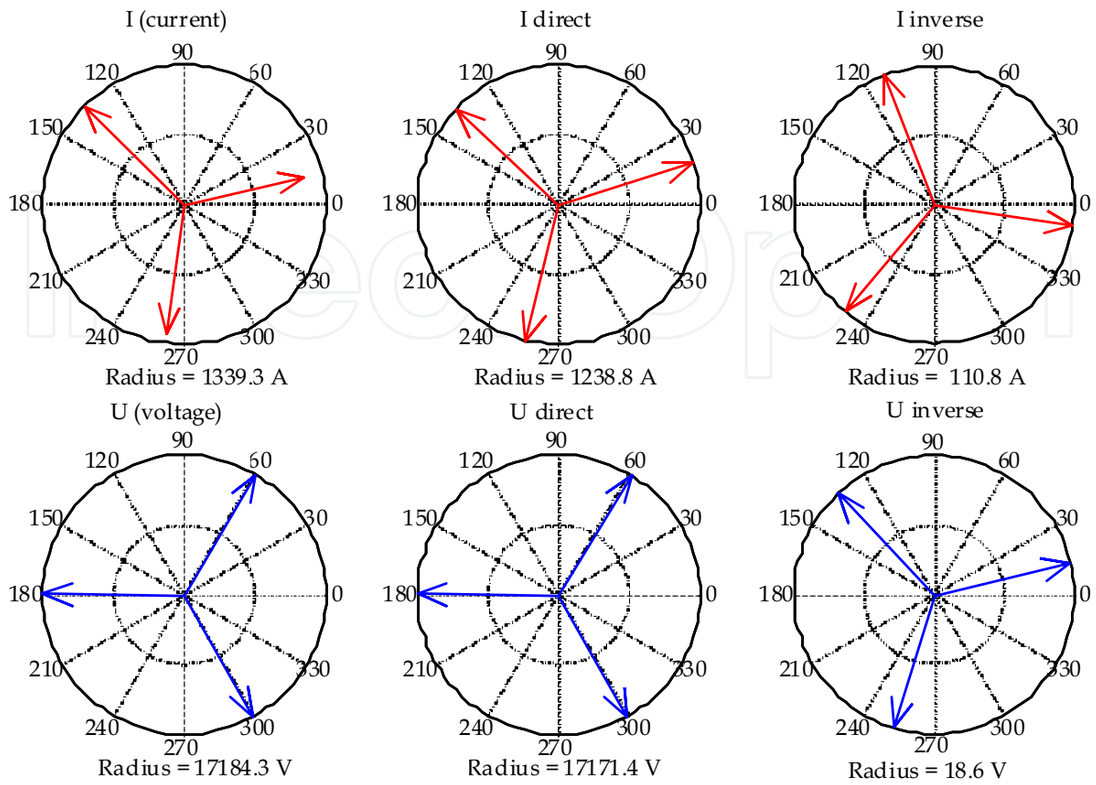


Fig. 13. Current and voltage phasors using only current harmonics filtering

### 4.5. Simulation results with reactive power compensation, load balancing and current harmonics filtering

From the previous presented is resulting that the performing of one single optimization action from the three ones is not fully advantageous. Thus, usually is eliminated the cause for which was applied the respective measure, while the other perturbation are emphasizing or does not modify. Neither the simultaneous approach of each two of the three aspects doesn't solve totally the problem because, usually, the elimination of two forms the perturbations leads to emphasize of the third.

The most favourable situation, that leads to optimization of the main operation regime, up to the one very close to the ideal one, is obtained obviously, by acting for the simultaneous solving of the three problems (Buta & Pană, 2000). This can be achieved by using of two compensators, one in Y connection and the other one in Δ connection. The first one is mandatory when is desired the filtration of the current harmonics and the second one for balancing. Each of them can fulfil also the compensation function of the reactive power on fundamental frequency. To be noticed, therefore, two designing possibilities of the two compensators, such as:

- Compensator Y fulfils both the filtration and compensation function of the reactive power on fundamental, up to the required level, and compensator Δ fulfils only the load balancing function. Compensation of the reactive power on fundamental will be achieved by the three-phase units of filter, designing of their component capacities being made in such

way that the sum of the reactive powers on the direct sequence component for the fundamental frequency to be exactly the reactive power necessary for compensation. This compensation solution is efficient in case of its application in grid sections with small load variations.

- Compensator Y is consisted from filtration units, symmetrically dimensioned, from the condition that the installed capacitive reactive power to be minimum, the Δ compensator having the function that, besides balancing, achieves also the rest of reactive power compensation on the direct sequence component for the fundamental frequency up to the desired level, aiming the improvement of the power factor or voltage adjustment. Due to the possibilities of achieving the Δ compensator with variable susceptances, this compensation solution presents a significantly higher flexibility and efficiency.

From theoretical viewpoint, the two designing methods are absolutely similar. Having in view the fact that the calculated installation is part of the first category, the performed analysis was achieved only for the first case. The results obtained in the case where it does intervene in all the three directions are presented in table 5.

| | ***The fundamental*** | ***5th harmonic*** | ***7th harmonic*** | ***11th harmonic*** | ***13th harmonic*** |
|---|---|---|---|---|---|
| $\underline{I}_R$ | 476.56-789.50 j | 4.15+6.64 j | 6.94+4.57 j | -3.25+0.90 j | -1.70+1.85 j |
| $I_R$ | 922.18 | 7.83 | 8.31 | 3.38 | 2.51 |
| $\underline{I}_S$ | -922.28-19.46 j | -4.70+1.81 j | -3.42-6.83 j | -0.35-0.93 j | 1.58-1.43 j |
| $I_S$ | 922.49 | 5.04 | 7.64 | 0.99 | 2.13 |
| $\underline{I}_T$ | 445.72+808.96 j | 0.55-8.45 j | -3.52+2.26 j | 3.61+0.03 j | 0.12-0.42 j |
| $I_T$ | 923.62 | 8.46 | 4.18 | 3.61 | 0.43 |
| $\underline{I}^+$ | 477.69-789.42 j | -0.91+2.00 j | 6.07+2.32 j | -1.32-0.74 j | -0.53+1.31 j |
| $I^+$ | 922.70 | 2.20 | 6.50 | 1.51 | 1.41 |
| $\underline{I}^-$ | -0.55-0.09 j | 4.70+4.64 j | 0.77+2.36 j | -1.89+1.57 j | -1.17+0.54 j |
| $I^-$ | 0.55 | 6.60 | 2.48 | 2.45 | 1.29 |
| $\underline{I}^0$ | (-4+6.2 j)e-013 | (-2.7+8 j)e-014 | (1.4+3 j)e-013 | (-2.9+3 j)e-013 | (2.7-0.5 j)e-013 |
| $I^0$ | 7.48873e-013 | 2.8905e-013 | 3.55604e-013 | 4.23877e-013 | 2.7628e-013 |
| $k_{ni}$ [%] | 0.06 | 300.76 | 38.17 | 162.29 | 91.53 |
| $k_{nu}$[%] | 0.00 | 296.36 | 37.83 | 159.13 | 90.89 |
| $\gamma_{IkR}$ | 0.99944 | 0.00848 | 0.00901 | 0.00366 | 0.00272 |
| $\gamma_{IkS}$ | 0.99977 | 0.00546 | 0.00828 | 0.00107 | 0.00231 |
| $\gamma_{IkT}$ | 1.00099 | 0.00917 | 0.00453 | 0.00391 | 0.00047 |
| $\gamma_{UkR}$ | 0.99999 | 0.00031 | 0.00042 | 0.00024 | 0.00020 |
| $\gamma_{UkS}$ | 1.00001 | 0.00020 | 0.00039 | 0.00007 | 0.00017 |
| $\gamma_{UkT}$ | 1.00000 | 0.00034 | 0.00022 | 0.00026 | 0.00003 |

Table 5. Simulation results using reactive power compensation, load balancing and current harmonics filtering.

Both from table 5 and from the graphical representation of the current and voltage phasors from figure 14 is note the following:

- It was achieved a good reactive power compensation, that results because the phase difference between the direct sequence phasors of the current and voltage for fundamental frequency is very small, these being practically in phase;

- the small value of the reverse sequence components for current and voltage shows that it was achieved a good balancing also. This process can be improved in case when the balancing installation elements are calculated as in paragraph 4.3, but as input values are considered the current and voltage values obtained following the reactive power compensation action;
- the small values of the harmonic currents presented in table 5 show that it was achieved a good filtration also;
- in generally, the quality of the electric power in the node in which was intervened is much improved.

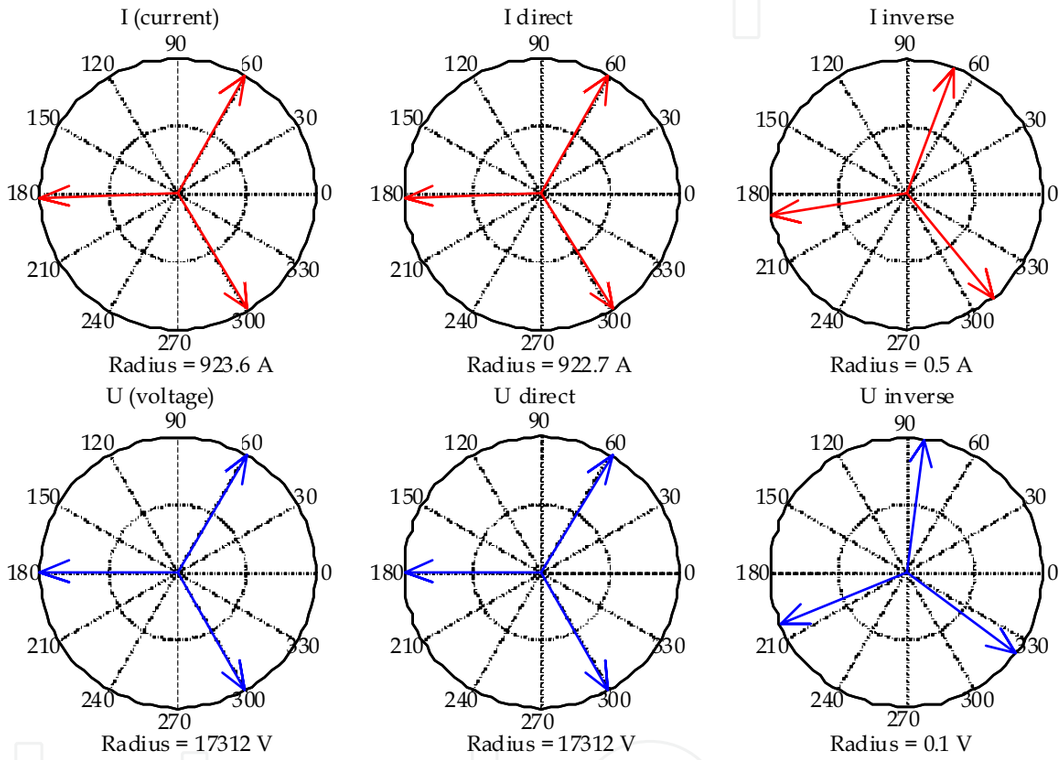


Fig. 14. Current and voltage phasors using reactive power compensation, load balancing g and current harmonics filtering

## 5. Conclusions

From the earlier presented simulations for the 5 cases presented were resulted conclusions referring to the obtained effects in increasing of the power quality in the node in which is acting. The most important indicators are presented in table 6.
Based on these results it can be concluded:

- in the situation in which is acting in only one action of increasing of power quality, the action has effects on reactive power circulation, on currents non-symmetry and non-sinusoidal regime. These effects are synthesized in table 7.

- In situation in which is acting in all three directions is obtaining the best improvement of the power quality in the node in which is acting.

| | | *Without any action* | *Only reactive power compensation* | *Only load balance* | *Only currents filtering* | *All three actions* |
|---|---|---|---|---|---|---|
| Y | C | – | 205,92 μF | – | – | 162,72 μF |
| | **L** | – | – | – | – | – |
| Δ | $\mathbf{C_{RS}}$ | – | – | 2,0675 μF | – | 2,0675 μF |
| | $\mathbf{C_{ST}}$ | – | – | 10,5931 μF | – | 10,5931 μF |
| | $\mathbf{L_{TR}}$ | – | – | 0,7824 H | – | 0,7824 H |
| | **U [V]** | 17219,4 | 17310,2 | 17219,2 | 17171,4 | 17312,2 |
| | $\mathbf{U_1}$ **[V]** | 17219,4 | 17310,2 | 17219,2 | 17171,4 | 17312,1 |
| | $\mathbf{U_k}$ **[V]** | 20,0996 | 22,1964 | 20,2206 | 25,4385 | 38,5512 |
| | **I [A]** | 1425,16 | 932,313 | 1422,1 | 1244,61 | 923,842 |
| | $\mathbf{I_1}$ **[A]** | 1423,76 | 929,741 | 1420,67 | 1244,09 | 922,762 |
| | $\mathbf{I_k}$ **[A]** | 63,17 | 69,199 | 63,7738 | 36,075 | 44,6559 |
| | $\underline{\mathbf{I}}^{+}$ **[A]** | -567,17-1300,31 j | 427,36-817,82 j | -568,51-1301,39 j | -276,93-1207,5 j | 477,69-789,42 j |
| | $\mathbf{I}^{+}$ **[A]** | 1418,62 | 922,75 | 1420,15 | 1238,86 | 922,70 |
| | $\underline{\mathbf{I}}^{-}$ **[A]** | 109,48-23,63 j | 109,57-24,91 j | 1,15+1,43 j | 109,48-17,23 j | -0,55-0,09 j |
| | $\mathbf{I}^{-}$ **[A]** | 112,00 | 112,37 | 1,83 | 110,83 | 0,55 |
| | $\mathbf{k_{ni}}$**[%]** | 7,90 | 12,18 | 0,13 | 8,95 | 0,06 |
| | $\mathbf{k_{nu}}$**[%]** | 0,05 | 0,05 | 0,00 | 0,11 | 0,00 |
| | $\mathbf{k_{ps}}$ | 0,645947 | 0,999684 | 0,645573 | 0,737698 | 0,99957 |
| | $\mathbf{k_{pn}}$ | -7,236e-006 | -9,967e-006 | -1,784e-008 | -1,317e-005 | -1,127e-009 |
| | $\mathbf{k_{pd}}$ | -9,481e-005 | -0,000177896 | -9,539e-005 | -2,494e-005 | -7,145e-005 |
| | $\mathbf{k_p}$ | 0,645845 | 0,999496 | 0,645478 | 0,73766 | 0,999499 |
| | **S[MVA]** | 73,621 | 48,416 | 73,462 | 64,115 | 47,981 |
| | $\mathbf{S_1}$**[MVA]** | 73,549 | 48,282 | 73,388 | 64,088 | 47,925 |
| | $\mathbf{S_k}$**[MVA]** | 3,264 | 3,594 | 3,296 | 1,861 | 2,322 |
| | **P[MW]** | 47,359 | 47,904 | 47,365 | 47,107 | 47,904 |
| | **Q[MVAR]** | 55,966 | -1,185 | 56,052 | 43,068 | -1,390 |
| | **D[MVAD]** | 6,708 | 6,919 | 3,379 | 6,072 | 2,342 |
| | **σ** | 1,25E-04 | 3,01e-009 | 6,27e-010 | 1,49e-009 | 1,02e-009 |
| | **Thdi** | 4,443 | 7,472 | 4,489 | 2,905 | 2,839 |
| | **Thdu** | 3,17 | 3,28 | 3,17 | 1,48 | 2,22 |
| | **Thdpi** | 11,117 | 18,966 | 11,255 | 6,625 | 5,891 |
| | **Thdpu** | 13,18 | 13,51 | 13,20 | 6,05 | 7,91 |

Table 6. Electrical installation simulation results depending on action of quality energy improvement.

| *Efect on: →*<br>*Action: ↓* | *Reactive power circulation* | *Unbalancing currents* | *Non sinusoidal regime* |
|---|---|---|---|
| **Reactive power compensation** | Eliminating | Accentuating | Accentuating |
| **Load balancing** | Not eliminating | Eliminating | Accentuating |
| **Harmonic currents filtering** | Reducing | Accentuating | Eliminating |

Table 7. Sinthesis of actions interdependency reffering to reactive power compensation, harmonic currents filtering and load balancing.

## 6. References


Andrews, D.; Bishop, M.T.; Witte, J.F. (1996). *Harmonic measurements, analysis and power factor correction in a modern steel manufacturing facility*, IEEE Transactions on Industry Applications, vol. 32, no. 3, May-June, pp. 617-624.

Boulet, B.; Lalli, G.; Agersch, M. (2003). *Modeling and Control of an Electric Arc Furnace*, Proceedings of the American Control Conference, Denver, Colorado, pp. 3060-3064.

Buta, A.; Pană, A.; Ivaşcu, C. (1997). *Reactive power compensation criteria in unbalanced electrical networks*, Energetica, vol. 45, pp. 289-294.

Buta, A.; Pană, A. (2000). *Simetrization of distribution electrical networks*, Technical Printing House, Timişoara.

Cano, P.E.A.; Tacca, H.E. (2005). *Arc Furnace Modeling in ATP-EMTP*, The 6th International Conference on Power Systems Transients (IPST), 19-23 June, Montreal, Canada.

Chiuță, I.; Conecini, I. (1989). *The compensation of the distorted functioning regime*, Technical Printing House, Bucureşti.

IEEE Standard 519-1992, "*IEEE Recommended Practices and Requirements for Harmonic Control in Electrical Power Systems,*" New York, 1992.

Ionescu, T.; Pop, O. (1998). *The power delivery engineering systems*, Technical Printing House, Bucureşti.

Montanari, G.C.; Loggini, M.; Cavallini, A.; Pitti, L.; Zaminelli, D. (1994). *Arc-Furnace model for the Study of Flicker Compensation in Electrical Networks,* IEEE Transactions on Power Delivery, vol. 9, no. 4, pp. 2026-2036.

Panoiu, M. (2001). *Some processes simulation based on three phase electric arc furnace modeling*, Ph.D. Thesis, Politechnical University of Timisoara, Romania.

Panoiu, M.; Panoiu, C. (2006). *Modeling and simulating the AC electric arc using PSCAD EMTDC,* Proceedings of the 5th WSEAS International Conference on System Science and Simulation in Engineering, Tenerife, Spain, 16-18 December.

Panoiu, M.; Panoiu, C.; Sora, I. (2006). *Experimental Research Concerning the Electromagnetic Pollution Generated by the 3-Phase Electric Arc Furnaces in the Electric Power Supply Networks*, Acta Electrotehnica, no. 2, vol 47, pp. 102-112.

Panoiu, M.; Panoiu, C. (2007). *Simulation Results for Modeling the AC Electric Arc as Nonlinear Element using PSCAD EMTDC*, WSEAS Transaction on Circuits and Systems, vol. 6, Jan, pp. 149-156.

Panoiu, M.; Panoiu, C.; Sora I. (2007). *Modeling Of Three Phase Electric Arc Furnaces*, Acta Electrotehnica, vol. 48, no. 2, pp. 124-132.

Panoiu, M.; Panoiu, C.; Sora, I.; Osaci, M. (2007). *Simulations Results on the Reactive Power Compensation Process on Electric Arc Furnace Using PSCAD-EMTDC*, International Journal of Modelling, Identification and Control, vol. 2, no. 3, , pp. 250-257.

Panoiu, M.; Panoiu; C.; Sora, I.; Osaci, M. (2007). *Using a Model Based on Linearization of the Current – Voltage Characteristic for Electric Arc Simulation*, Proceedings of the 16th IASTED International Conference on Applied Simulation and Modelling ~ASM 2007~ , Palma de Mallorca, Spain, August 29 – 31, pp. 99-103, ISBN 978-0-88986-687-4, Acta Press Printing House.

Panoiu, M.; Panoiu, C.; Sora, I.; Osaci, M. (2007). *About the possibility of power controlling in the Three-Phase Electric Arc Furnaces using PSCAD EMTDC simulation program*, Advances in Electrical and Computer Engineering , vol. 7, number 1 (27), ISSN 1582-7445, pp. 38-43.

Panoiu, M.; Panoiu, C.; Sora, I.; Osaci, M.; Muscalagiu, I. (2007). *Modeling, Simulating and Experimental Validation of the AC Electric Arc in the Circuit of Three-Phase Electric Furnaces*, EUROSIM 2007 Congress, Ljubljana, Slovenia, Book of Abstract, pp. 241, CD-Proceedings, 10 pg., ISBN 3-901608-32-x, CD-Proceedings, ISBN 987-33-901608-32-2.

Tang, L.; Kolluri, S.; Mark, F. Mc-Granaghan. (1997). *Voltage Flicker Prediction for two simultaneously operated Arc Furnaces*, IEEE Transactions on Power Delivery, vol. 12, no. 2.

Wu, C. J.; Huang, C. P.; Fu T. H.; Zhao, T. C.; Kuo, H. S. (2002). *Power factor definitions and effect on revenue of electric arc furnace load*, International Conference on Power System Technology Proceedings, vol. 1, pp. 93-97.

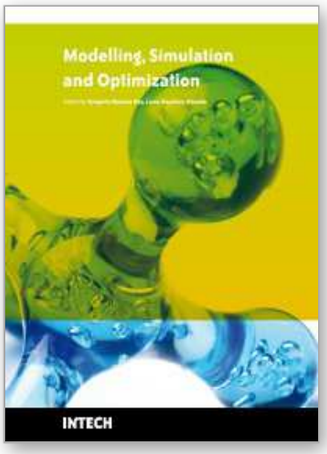


**Modelling Simulation and Optimization**

Edited by Gregorio Romero Rey and Luisa Martinez Muneta

ISBN 978-953-307-048-3
Hard cover, 708 pages
**Publisher** InTech
**Published online** 01, February, 2010
**Published in print edition** February, 2010

Computer-Aided Design and system analysis aim to find mathematical models that allow emulating the behaviour of components and facilities. The high competitiveness in industry, the little time available for product development and the high cost in terms of time and money of producing the initial prototypes means that the computer-aided design and analysis of products are taking on major importance. On the other hand, in most areas of engineering the components of a system are interconnected and belong to different domains of physics (mechanics, electrics, hydraulics, thermal...). When developing a complete multidisciplinary system, it needs to integrate a design procedure to ensure that it will be successfully achieved. Engineering systems require an analysis of their dynamic behaviour (evolution over time or path of their different variables). The purpose of modelling and simulating dynamic systems is to generate a set of algebraic and differential equations or a mathematical model. In order to perform rapid product optimisation iterations, the models must be formulated and evaluated in the most efficient way. Automated environments contribute to this. One of the pioneers of simulation technology in medicine defines simulation as a technique, not a technology, that replaces real experiences with guided experiences reproducing important aspects of the real world in a fully interactive fashion [iii]. In the following chapters the reader will be introduced to the world of simulation in topics of current interest such as medicine, military purposes and their use in industry for diverse applications that range from the use of networks to combining thermal, chemical or electrical aspects, among others. We hope that after reading the different sections of this book we will have succeeded in bringing across what the scientific community is doing in the field of simulation and that it will be to your interest and liking. Lastly, we would like to thank all the authors for their excellent contributions in the different areas of simulation.

Slavka Krautzeka 83/A
51000 Rijeka, Croatia
Phone: +385 (51) 770 447
Fax: +385 (51) 686 166
www.intechopen.com

No.65, Yan An Road (West), Shanghai, 200040, China
中国上海市延安西路65号上海国际贵都大饭店办公楼405单元
Phone: +86-21-62489820
Fax: +86-21-62489821



IntechOpen

IntechOpen